Atmos. Meas. Tech. Discuss., https://doi.org/10.5194/amt-2017-484
Manuscript under review for journal Atmos. Meas. Tech.
Discussion started: 30 January 2018

Atmospheric Measurement Techniques
Discussions

Potential sources of a priori ozone profiles for TEMPO tropospheric ozone retrievals

Matthew S. Johnson[1], Xiong Liu[2], Peter Zoogman[2,*], John Sullivan[3], Michael J. Newchurch[4], Shi Kuang[5], Thierry Leblanc[6], Thomas McGee[3]

[1]Earth Science Division, NASA Ames Research Center, Moffett Field, CA, USA.
[2]Harvard-Smithsonian Center for Astrophysics, Cambridge, MA, USA.
[3]Atmospheric Chemistry and Dynamics Laboratory, NASA Goddard Space Flight Center, Greenbelt, Maryland, USA.
[4]Atmospheric Science Department, University of Alabama in Huntsville, Huntsville, AL, USA.
[5]Earth System Science Center, University of Alabama in Huntsville, Huntsville, AL, USA.
[6]Table Mountain Facility, California Institute of Technology, Wrightwood, CA, USA.
*also at Minerva Schools at KGI, San Francisco, CA, USA.

Correspondence to: Matthew S. Johnson (matthew.s.johnson@nasa.gov)

Abstract. Potential sources of a priori ozone (O_3) profiles for use in Tropospheric Emissions: Monitoring of Pollution (TEMPO) satellite tropospheric O_3 retrievals are evaluated with observations from multiple Tropospheric Ozone Lidar Network (TOLNet) systems in North America. An O_3 profile climatology (tropopause-based O_3 climatology (TB-Clim), currently proposed for use in TEMPO O_3 retrieval algorithms) based on ozonesonde observations and O_3 profiles from three separate models (operational Goddard Earth Observing System (GEOS-5) Forward Processing (FP) product, reanalysis product from Modern-Era Retrospective analysis for Research and Applications version 2 (MERRA2), and the GEOS-Chem chemical transport model (CTM)) were: 1) evaluated with TOLNet measurements on various temporal scales (seasonally, daily, hourly) and 2) implemented as a priori information in theoretical TEMPO tropospheric O_3 retrievals in order to determine how each a priori impacts the accuracy of retrieved tropospheric (0-10 km) and lowermost tropospheric (LMT, 0-2 km) O_3 columns. We found that all potential sources of a priori profiles evaluated in this study generally reproduced the vertical structure of summer-averaged observations of O_3 profiles. However, larger differences between the a priori profiles and lidar observations were observed when evaluating inter-daily and diurnal variability of tropospheric O_3. The TB-Clim O_3 profile climatology was unable to replicate observed inter-daily and diurnal variability of O_3 while model products, in particular GEOS-Chem simulations, displayed more skill in reproducing these features. Due to the ability of models, primarily the CTM used in this study, on average to capture the inter-daily and diurnal variability of tropospheric and LMT O_3 columns, using a priori profiles from these model simulations resulted in TEMPO retrievals with the best statistical comparison with lidar observations. Furthermore, important from an air quality perspective, when high LMT O_3 values are observed, using GEOS-Chem a priori profiles resulted in TEMPO LMT O_3 retrievals with the least bias.

1 Introduction

Ozone (O_3) is an important atmospheric constituent for air quality as concentrations above natural levels can have detrimental health impacts (US EPA, 2006) and the United States (US) Environmental Protection Agency (EPA) enforces surface-level mixing ratios under the National Ambient Air Quality Standards (NAAQS). In 2015, the

NAAQS for O_3 was reduced from prior levels of 75 parts per billion (ppb) to 70 ppb, requiring that 3-year averages of the annual fourth-highest daily maximum 8-hour mean mixing ratio must be ≤ 70 ppb (US EPA, 2015). Tropospheric and surface-level O_3 mixing ratios are controlled by a complex system of photo-chemical reactions involving numerous trace gas species (e.g., carbon monoxide (CO), methane, volatile organic compounds, and nitrogen oxides (NO_x = nitric oxide and nitrogen dioxide ($NO + NO_2$)) emitted from anthropogenic and natural sources (Atkinson, 1990; Lelieveld and Dentener, 2000). Furthermore, a portion of tropospheric O_3 is also contributed from the downward transport from the stratosphere, commonly referred to as stratosphere-to-troposphere exchange (STE) (e.g., Stohl et al., 2003; Lin et al., 2015). Due to the complex chemistry and transport processes controlling O_3 mixing ratios, and the continued reduction of NAAQS levels, it is increasingly important to improve the ability to monitor/study tropospheric and surface-level O_3.

The monitoring of air quality in North America is typically conducted by using ground-based in situ measurement networks. However, in recent years, observations of tropospheric O_3 and precursor gases (e.g., CO, NO_2, formaldehyde (HCHO)) have been made from space-borne platforms which have led to the better understanding of the tropospheric O_3 budget (Sauvage et al., 2007; Martin, 2008; Duncan et al., 2014). Total column (stratosphere + troposphere) O_3 has been routinely measured by numerous space-based sensors since the launch of the Total Ozone Mapping Spectrometer (TOMS) in 1978. Tropospheric column O_3 has been derived from total column retrievals using strategies such as residual-based approaches which subtract the stratospheric column O_3 from total O_3 (Fishman et al., 2008 and references therein). Tropospheric O_3 profiles have also been directly retrieved from hyperspectral Ultraviolet (UV) (e.g., Liu et al., 2005, 2010) and Thermal Infrared (TIR) (e.g., Bowman et al., 2006) measurements. Currently, sensors measuring tropospheric O_3, such as those using UV measurements from the Ozone Monitoring Instrument (OMI) and TIR measurements from the Tropospheric Emission Spectrometer (TES) (Beer, 2006), are from low earth orbit (LEO). While LEO provides global coverage, the observation of tropospheric O_3 is limited by coarse spatial resolution, limited temporal frequency (once or twice per day), and inadequate sensitivity to lower tropospheric and planetary boundary layer (PBL) O_3 (Fishman et al., 2008; Natraj et al., 2011). These limitations restrict the ability to apply these space-borne observations in air quality policy and monitoring.

The Tropospheric Emissions: Monitoring of Pollution (TEMPO) satellite, which will be launched between 2019-2021 to geostationary orbit (GEO), is designed to address some of the limitations of current O_3 remote-sensing instruments (Chance et al., 2013; Zoogman et al., 2017). TEMPO will provide critical measurements such as vertical profiles of O_3, total column O_3, NO_2, sulfur dioxide, HCHO, glyoxal, and aerosol/cloud parameters over North America. These data products will be provided hourly at a native spatial resolution of ~2.1×4.4 km^2 (at the center of the field of regard) except at the required spatial resolution of 8.4×4.4 km^2 for the O_3 profile product (four pixels combined to increase signal to noise ratios and reduce computational resources). TEMPO's domain will encompass the region of North America from Mexico City to the Canadian oil sands and from the Atlantic to the Pacific Ocean. TEMPO will have increased sensitivity to lower tropospheric O_3 compared to past/current satellite data by combining measurements from both UV (290-345 nm) and visible (VIS, 540-650 nm) wavelengths (Natraj et al., 2011; Zoogman et al., 2017). The operational TEMPO O_3 product will provide vertical profiles and partial O_3 columns at ~24-30 layers from the surface to ~60 km above ground level. This product will also include total, stratospheric, tropospheric, and a

Atmos. Meas. Tech. Discuss., https://doi.org/10.5194/amt-2017-484
Manuscript under review for journal Atmos. Meas. Tech.
Discussion started: 30 January 2018

Atmospheric Measurement Techniques Discussions

0-2 km above ground level O_3 columns. TEMPO's high spatial and temporal resolution measurements, including the 0-2 km O_3 column, will provide a wealth of information to be used in air quality monitoring and research.

Vertical O_3 profile retrievals from TEMPO will be based on the Smithsonian Astrophysical Observatory (SAO) O_3 profile algorithm which was developed for use in the Global Ozone Monitoring Experiment (GOME) (Liu et al., 2005), OMI (Liu et al., 2010), GOME-2 (Cai et al., 2012), and the Ozone Mapping and Profiler Suite (Bak et al., 2017). The SAO O_3 algorithm for TEMPO will apply the tropopause-based O_3 climatology (TB-Clim) developed in Bak et al. (2013) as the a priori profiles, which was demonstrated to improve OMI O_3 retrievals near the tropopause compared to calculations using the Labow-Logan-McPeters (LLM) O_3 climatology (a priori used for OMI) (McPeters et al., 2007). During this work, we evaluate the representativeness of the vertical O_3 profiles from TB-Clim. Additionally, we evaluate simulated O_3 profiles from a near-real-time (NRT) data assimilation model product (National Aeronautics and Space Administration (NASA) Global Modeling and Assimilation Office (GMAO) Goddard Earth Observing System (GEOS-5) Forward Processing (FP)), a reanalysis data product (NASA GMAO Modern-Era Retrospective analysis for Research and Applications version 2 (MERRA2)), and a chemical transport model (CTM) (GEOS-Chem). The climatology and model O_3 profiles were evaluated with ground-based lidar data from the Tropospheric Ozone Lidar Network (TOLNet) at various locations of the US during the summer of 2014. This evaluation was focused on the performance of each product compared to summer-, daily-, and hourly-averaged lowermost tropospheric (LMT, 0-2 km) and tropospheric (0-10 km) O_3 columns to demonstrate the effectiveness of using the TB-Clim and additional products as a priori in the TEMPO O_3 profile algorithm.

This paper is organized as follows. Section 2 describes the tropospheric lidar O_3 measurements, TB-Clim and model products, theoretical TEMPO retrievals, and data evaluation techniques applied during this study. Section 3 provides the results of the comparison of the TB-Clim and modeled a priori profile products with TOLNet observations and the impact of each product, when applied as a priori, on TEMPO tropospheric O_3 profile retrievals. Finally, Sect. 4 concludes this study.

2 Data and methods

2.1 TOLNet

TOLNet provides Differential Absorption Lidar (DIAL)-derived vertically-resolved O_3 mixing ratios at 6 different locations of North America (http://www-air.larc.nasa.gov/missions/TOLNet/). TOLNet data have been used extensively in atmospheric chemistry research on topics such as STE, air pollution transport, nocturnal O_3 enhancements, PBL pollution entrainment, source attribution of O_3 lamina, and the impact of wildfire and lightning NO_x on tropospheric O_3 (e.g., Kuang et al., 2011; Sullivan et al., 2015a, Johnson et al., 2016; Granados-Muñoz et al., 2017; Langford et al., 2017). Past analysis has demonstrated the high accuracy of TOLNet O_3 retrievals with errors typically estimated to be around ±10% in the lower troposphere and ±20% in the upper troposphere (Kuang et al., 2013; Sullivan et al., 2015b; Granados-Muñoz and Leblanc, 2016). TOLNet data will be applied in this study to evaluate the TB-Clim and model-predicted profiles which could potentially be used as TEMPO a priori information. Furthermore, theoretical TEMPO O_3 retrievals in the troposphere and LMT were calculated using the climatology/model profiles as a priori with TOLNet data representing the “true” atmospheric O_3 profiles (see Sect. 2.2).

During this study, vertical O_3 profiles from 3 separate TOLNet sites during the summer (July-August) of 2014 were applied. Figure 1 shows the location of the Goddard Space Flight Center (GSFC) TROPospheric OZone (TROPOZ), Jet Propulsion Laboratory (JPL) Table Mountain Facility (TMF), and the University of Alabama in Huntsville (UAH) Rocket-city O_3 Quality Evaluation in the Troposphere (RO3QET) TOLNet systems which provided the observations used during this work. These 3 sites were selected due to data availability (http://www-air.larc.nasa.gov/missions/TOLNet/data.html) and to represent differing parts of North America, which will be observed by TEMPO, with varying topography, meteorology, and atmospheric chemistry conditions (overview information for each station is presented in Table 1). The RO3QET system is located in the southeast US where the air quality is impacted by both anthropogenic and natural emission sources, complex chemistry, and multiple transport pathways (e.g., Hidy et al., 2014; Johnson et al., 2016; Kuang et al., 2017). During the summer of 2014 this lidar system measured O_3 profiles from the surface to ~5 km above ground level during the daytime hours. The TROPOZ system, which is typically operated at NASA GSFC, was remotely stationed in Colorado to support the Deriving Information on Surface Conditions from COlumn and VERtically Resolved Observations Relevant to Air Quality (DISCOVER-AQ) Colorado and Front Range Air Pollution and Photochemistry Éxperiment (FRAPPÉ) field campaigns between July-August 2014. The TROPOZ system was arranged to take daytime observations of O_3 profiles in the intermountain west region of the US alongside the frontal range of the Rocky Mountains. The air quality of this location is impacted by large anthropogenic emission sources, complex local transport, and common STE events (e.g., Sullivan et al., 2015a; Vu et al., 2016). Finally, the TOLNet system at the JPL TMF is representative of the western US and remote high-elevation locations. This location has O_3 profiles largely controlled by long-range transport and STEs typical of remote high-elevation locations in the US (e.g., Granados-Muñoz and Leblanc, 2016; Granados-Muñoz et al., 2017). During the summer of 2014, the JPL TMF lidar only conducted measurements during the nighttime hours and therefore will only be used for daily-averaged comparisons to TB-Clim and model predictions.

2.2 TEMPO O_3 profile retrieval

TEMPO will adapt the current SAO OMI UV-only O_3 profile algorithm (Liu et al., 2010) to derive O_3 profiles from joint UV+VIS measurements based on the optimal estimation technique (Rodgers, 2000). Partial O_3 columns at different altitudes, along with other retrieved variables, are iteratively derived by simultaneously minimizing the differences between measured and simulated radiances and between the retrieved and a priori state vectors. For this study, we use the linear estimate approach to perform theoretical TEMPO retrievals and evaluate the impact of a priori profiles on these retrievals. This linear estimation approach is a good approximation of the non-linear retrieval and has been used in past research (e.g., Natraj et al., 2011). In this approach, shown in Eq. (1), the retrieved O_3 profile (X_r) is derived as:

$$X_r = X_a + A(X_t - X_a) + G\varepsilon, \tag{1}$$

where X_a is the a priori O_3 profile, A is the averaging kernel (AK) matrix, X_t is the true O_3 profile, G is the gain matrix, and ε is the measurement noise.

Atmos. Meas. Tech. Discuss., https://doi.org/10.5194/amt-2017-484
Manuscript under review for journal Atmos. Meas. Tech.
Discussion started: 30 January 2018

2.2.1 TEMPO averaging kernels

The UV+VIS AKs applied during this study are based on TEMPO retrieval sensitivity studies that play a key role in determining the instrument requirements and verification of the retrieval performance (Zoogman et al., 2017). The production of these AKs involved: 1) radiative transfer model simulations of TEMPO radiance spectra and weighting functions, 2) retrieval AKs and errors constrained by the TB-Clim a priori error covariance matrix, and 3) measurement errors estimated using the TEMPO signal to noise ratio model. To represent TEMPO hourly measurements throughout the year, the retrieval sensitivity calculation was performed hourly for 12 days (15th day of each month) over the TEMPO domain at a spatial resolution of 2.0°×2.5° (latitude × longitude) using hourly GEOS-Chem model fields. During this study, we use the UV+VIS O_3 retrieval AKs corresponding to the month and location of TOLNet systems representative of near clear-sky conditions. Figure 2 shows an example of the UV+VIS AK matrix at the UAH RO3QET site for 20 UTC in August. The enhanced sensitivity of TEMPO retrievals in the lower troposphere, in particular the lowest ~2 km, is demonstrated by the large values of A (normalized to 1 km, degrees of freedom (DFS) per km) in Fig. 2 (> 0.20). When including VIS with UV wavelengths, O_3 retrievals can be greater than a factor of 2 more sensitive in the first 2 km of the troposphere in comparison to just using UV wavelengths. This is particularly important as accurate O_3 observations between 0-2 km above the surface is a key requirement of TEMPO to be a sufficient data source for air quality research/monitoring (Zoogman et al., 2017).

2.2.2 TB-Clim

During this study, TB-Clim is evaluated with observations to determine the ability of these profiles to represent the spatio-temporal variability of tropospheric O_3 in North America. A detailed description of the data and procedures used to derive TB-Clim can be found in Bak et al. (2013). The climatology provides monthly-averaged O_3 profiles with 1 km vertical resolution relative to the tropopause in 18 10°-latitude bins (Bak et al., 2013). During this study, hourly TB-Clim O_3 profiles were derived by applying hourly-averaged GEOS-5 FP tropopause heights. Figure 3 illustrates the monthly-averaged vertical structure of TB-Clim that will be evaluated at the RO3QET, TROPOZ, and JPL TMF system locations representative of various regions of the US in July-August 2014. At the location of the RO3QET system (Fig. 3, yellow line), O_3 values are ~55 ppb near the surface during July and August and steadily increase to ~95 ppb at 10 km. For the location of the TROPOZ system (Fig. 3, black line), O_3 values are ~40-45 ppb near the surface and increase to ~80 ppb at 10 km. Finally, at the location of the JPL TMF lidar system (Fig. 3, red line), O_3 values are ~50-55 ppb near the surface and increase to 80-95 ppb at 10 km.

2.3 Simulated O_3 profile data

Satellite O_3 retrieval algorithms typically apply climatologies derived from observational data (i.e., ozonesondes) as a priori information (Liu et al., 2005, 2010; Cai et al., 2012). However, some satellites, such as TES operational retrievals, apply climatological O_3 profiles from global CTMs as a priori information (Worden et al., 2007). During this work, we evaluate O_3 profile information from a NRT operational data assimilation model (GEOS-5 FP), reanalysis model (MERRA2), and a CTM (GEOS-Chem) using TOLNet data and investigate how model products impact theoretical TEMPO O_3 retrievals when applied as a priori information. These simulated products were selected to represent model predictions of O_3 with highly varying complexity in atmospheric chemistry calculations, emissions information, data assimilation techniques, and spatial resolution.

2.3.1 GEOS-5 FP and MERRA2

The GEOS-5 atmospheric general circulation model (AGCM) and data assimilation system (DAS) is a product of the GMAO and is described in Rienecker et al. (2008) with most recent updates presented in Molod et al. (2012). Aerosol and trace gases are transported in the GEOS-5 AGCM using a finite-volume dynamics scheme implemented with various physics packages (Putman and Lin, 2007; Bacmeister et al., 2006) and turbulently mixed using the Lock et al. (2000) PBL scheme. The GEOS-5 AGCM ADS assimilates roughly 2×10^6 observations for each analysis using the Gridpoint Statistical Interpolation (GSI) three dimensional variational (3DVar) analysis technique (Wu et al., 2002). A product from the GEOS-5 AGCM is the operationally provided GEOS-5 FP data which offers NRT DAS predictions (typically within 24 hours) of O_3 vertical profiles at a 0.25°×0.3125° spatial resolution and 72 vertical levels. Additionally, we apply MERRA2 reanalysis O_3 profiles which are also produced using the GEOS-5 AGCM (Molod et al., 2012) and provided at a 0.50°×0.667° spatial resolution and 72 vertical levels. Both GEOS-5 FP and MERRA2 O_3 vertical profiles are driven by the assimilation of OMI and Microwave Limb Sounder (MLS) satellite data. Predictions of O_3 from these products are most trusted in the upper troposphere and stratosphere due to data constraints predominantly occurring in these altitude ranges (e.g., Wargan et al., 2015; Ott et al., 2016). The work by Wargan et al. (2015) shows that due to highly simplified atmospheric chemistry and lack of surface emissions in the GEOS-5 AGCM, O_3 predictions in the middle to lower troposphere tend to be biased. However, during this work these 3 hour-averaged products are applied to understand how NRT DAS and reanalysis models could be used as a priori information in TEMPO O_3 retrievals.

2.3.2 GEOS-Chem

GEOS-Chem (v9-02) was applied in this work as a proxy to determine how a full CTM or air quality model could potentially be used as a priori information in TEMPO O_3 retrieval algorithms. The purpose of this work is not to evaluate the performance of the GEOS-Chem model, or to suggest GEOS-Chem as the only model to provide a priori information for TEMPO, but to simply evaluate how CTM predictions impact the accuracy of theoretical TEMPO O_3 retrievals. The CTM is driven by GEOS-5 FP meteorological data in a nested regional mode for July and August 2014, after a 2-month spin-up period, at a 0.25°×0.3125° spatial resolution and 47 hybrid terrain following vertical levels for the North American domain (130°-60°W, 9.75°-60°N). GEOS-Chem includes detailed O_3-NO_x-hydrocarbon-aerosol chemistry coupled to H_2SO_4-HNO_3-NH_3 aerosol thermodynamics (Bey et al., 2001). Furthermore, aerosol and trace gas transport are calculated using the TPCORE parameterization (Lin and Rood, 1996) and dry and wet deposition (Wang et al., 1998; Amos et al., 2012) is simulated on a 10-minute time-step. A detailed description of the version of GEOS-Chem, and emission inventories, applied during this study can be found in Johnson et al. (2016).

2.4 Data evaluation

The evaluation of TB-Clim and model O_3 profiles was done for summer-, daytime- (6am - 6pm local time), and hourly-averages at the RO3QET and TROPOZ system locations during July and August 2014. Due to the hours of operation, the evaluation at the JPL TMF lidar location was conducted for summer- and daily-averages. To determine the ability of a NRT DAS, reanalysis, and CTM model to replicate TOLNet-observed O_3, GEOS-5 FP, MERRA2, and GEOS-Chem data will be evaluated simultaneously with TB-Clim. For all evaluation and inter-comparisons, TB-Clim, model data, TOLNet observations, and TEMPO calculations are hourly-averaged and averaged/interpolated to the vertical grid of the TEMPO AKs during all times/locations when/where TOLNet measurements were obtained. TB-Clim and model data used as a priori and resulting X_r calculations will be evaluated using statistical parameters (correlation (R), bias, bias standard deviation (1σ), mean normalized bias (MNB), root mean squared error (RMSE)) and time-series analysis for tropospheric (0-10 km, 0-5 km for RO3QET) and LMT (0-2 km) columns. Tropospheric column values are considered to extend from the surface to 10 km in this study based on the fact that TOLNet systems typically only measured to ~10 km.

3 Results

3.1 Evaluation of TB-Clim and model-predicted tropospheric O_3 profiles

In terms of summertime-averaged tropospheric O_3 profiles, TB-Clim and the GEOS-5 FP, MERRA2, and GEOS-Chem models could generally replicate the vertical structure of tropospheric O_3 measured by TOLNet lidars. However, the evaluation of these products as a priori in TEMPO O_3 retrievals at a seasonal/monthly average is insufficient as TEMPO will provide hourly, high spatial resolution, tropospheric and LMT O_3 values. Therefore, in the following sections we evaluate these products for daily- and hourly-averages to focus on inter-daily and diurnal variability.

3.1.1 Daily-averaged tropospheric O_3 profiles

This section focuses on evaluating the ability of TB-Clim and the GEOS-5 FP, MERRA2, and GEOS-Chem models to reproduce observed daily variability of O_3 in the troposphere and near the surface. Figure 4 shows the daily-averaged tropospheric and LMT O_3 columns from TB-Clim and models compared to that observed by TOLNet at all 3 sites with comparison statistics displayed in Table 2. Some slight inter-daily variability can be seen in TB-Clim tropospheric O_3 due to varying time-dependent tropopause heights, however, the variability in LMT values is mostly due to only sampling values in the vertical layers and times when TOLNet observations were obtained (vertical layers of TOLNet observations varied between hours and days). Due to the zonal and monthly mean nature of TB-Clim, this dataset is unable to replicate inter-daily O_3 observations consistently displaying negative correlation values with daily TOLNet observations in the troposphere (R range between -0.09 and -0.35) and near the surface (R range between -0.15 and -0.68). The models demonstrate a better ability to replicate the daily variability of observed tropospheric O_3 at the TOLNet system locations. Overall, CTM predictions from GEOS-Chem was the only potential source of a priori profiles which consistently displayed moderate to high positive correlation (all R values > 0.47) compared to all TOLNet observations in the troposphere and near the surface. This result is not overly surprising as a full CTM includes aspects necessary to reproduce the spatio-temporal tropospheric O_3 variability occurring in nature such as data-assimilated meteorological fields, comprehensive atmospheric chemistry mechanisms, and state-of-the-art trace gas and aerosol emissions data.

Figure 4a, b shows larger variability of daily-averaged LMT O_3 (44 to 68 ppb) from the RO3QET system than that in the tropospheric column (48 to 64 ppb). From Table 2 it can be seen that TB-Clim was generally high compared to lidar-measured tropospheric O_3 mixing ratios (average bias = 3.7 ppb) with large bias standard deviations and RMSE values (> 6 ppb). MERRA2 displayed good agreement in tropospheric O_3 (negative bias ~0.7 ppb) while GEOS-5 FP and GEOS-Chem resulted in moderate high biases (average bias 2.8 and 1.7 ppb, respectively). GEOS-Chem had moderate high biases but with smaller bias standard deviation and RMSE values (< 4.5 ppb) in comparison to the other products due to the ability to better capture inter-daily tropospheric O_3 variability (R = 0.61). LMT O_3 observations by the RO3QET lidar were best replicated by the CTM product resulting in the smallest average bias (-1.3 ppb) and bias standard deviation and RMSE values (4.4 ppb) compared to the other products. MERRA2 was consistently low compared to LMT O_3 observations (bias = -4.9 ppb) while TB-Clim and GEOS-5 FP resulted in moderate biases (2.9 and -2.9 ppb, respectively) with all of these products having large bias standard deviations and RMSE (≥ 8.0 ppb).

At the TROPOZ system location, large variability in tropospheric (47 to 83 ppb) and LMT O_3 values (41 to 73 ppb) was observed. From Fig. 4c, d and Table 2 it can be seen that TB-Clim is unable to replicate the inter-daily tropospheric O_3 variability and is generally higher in comparison to observations with large bias standard deviations (bias ± standard deviation = 2.2 ± 9.7 ppb). GEOS-Chem best replicates the daily variability of tropospheric O_3 with the largest correlation (R = 0.82) and small average bias and standard deviations (2.4 ± 6.0 ppb). GEOS-5 FP and MERRA2 data displayed low positive correlations (R < 0.40) and larger average biases and standard deviations 3.3 ± 10.0 and -4.6 ± 9.1 ppb, respectively. In comparison to TROPOZ LMT O_3 observations, TB-Clim and all model products displayed large negative biases. The TB-Clim product resulted in the largest negative biases and bias standard deviations compared to LMT O_3 observations (-11.1 ± 7.5 ppb) and model products displayed smaller biases and standard deviations. GEOS-5 FP data displayed the lowest average bias (-4.4 ppb) compared to TROPOZ observations, however, was unable to replicate the inter-daily variability of LMT O_3 (R = -0.09) resulting in large bias standard deviations (7.3 ppb). Overall, GEOS-Chem was the only product which was able to capture the inter-daily variability of LMT O_3 (R = 0.47) resulting in moderate low biases and the lowest bias standard deviation (-6.7 ± 6.2 ppb).

Figure 4e, f illustrates that large inter-daily variability of tropospheric (46 to 129 ppb) and LMT (35 to 76 ppb) column O_3 was observed at the JPL TMF site during the summer of 2014. This figure and Table 2 shows that TB-Clim is able to represent the average magnitude of tropospheric O_3 (bias = 0.3 ppb) but with large bias standard deviation and RMSE values (>18 ppb) due to the inability to replicate observed inter-daily variability (R = -0.35). The GEOS-Chem model also captures the average magnitude of tropospheric O_3 (bias = -0.5 ppb) but with smaller bias standard deviations (14.6 ppb) compared to TB-Clim due to the ability to replicate the inter-daily availability (R = 0.72). GEOS-5 FP and MERRA2 demonstrated negative biases compared to JPL TMF lidar observed tropospheric O_3 (-5.0 and -10.6 ppb, respectively) with relatively low bias standard deviations (~13-14 ppb) compared to the other products. The large RMSE values for all products is due to the very large variability in daily-averaged O_3 observations which was not well captured by all products. Near the surface, the GEOS-Chem model clearly best captures the variability of daily-averaged LMT O_3 indicated by the smallest bias and standard deviations (0.9 ± 10.4 ppb) and RMSE (~10.25 ppb) values.

3.1.2 Diurnal cycle of tropospheric O_3 profiles

TEMPO retrievals will produce hourly tropospheric and LMT O_3 values each day for the entire North America domain. Therefore, this section focuses on evaluating the ability of TB-Clim and the GEOS-5 FP, MERRA2, and GEOS-Chem models to reproduce the observed diurnal variability of O_3 measured at the RO3QET and TROPOZ system locations in the troposphere and near the surface. Figure 5 shows the average diurnal time-series of hourly-averaged tropospheric and LMT O_3 (from all days of observation) from the O_3 climatology and models compared to that observed during the summer of 2014 (statistics displayed in Table 3).

Figure 5a, b shows that larger diurnal variability of O_3 was observed for LMT values (48 to 59 ppb) compared to tropospheric values (55 to 60 ppb) at the RO3QET lidar location. All the potential sources of a priori profiles, excluding the CTM predictions, demonstrate very little diurnal variation in tropospheric and LMT O_3 at the RO3QET lidar location during the summer of 2014. The GEOS-Chem model was the only product able to replicate the diurnal variability of observed tropospheric O_3 (R = 0.68). MERRA2 resulted in the lowest bias (-1.2 ppb), GEOS-5 FP and GEOS-Chem displayed modest biases (~2.0-2.5 ppb), and TB-Clim had the largest bias (3.5 ppb) compared to RO3QET tropospheric O_3 data. Diurnal RO3QET LMT O_3 data was best replicated by CTM predictions resulting in the highest correlation (R = 0.76), lowest bias and standard deviations (0.3 ± 2.6 ppb), and RMSE values (2.45 ppb). The TB-Clim product resulted in modest biases compared to LMT O_3 data (1.9 ppb) while GEOS-5 FP and MERRA2 were consistently low (negative bias > 3.0 ppb).

Figure 5c, d shows the diurnal variability of O_3 that was observed for tropospheric and LMT column values at the TROPOZ lidar location during the summer of 2014. In the troposphere, O_3 values varied between ~58 to 69 ppb with largest values occurring in the afternoon. Larger diurnal variability was observed near the surface with LMT O_3 values ranging from ~56 to 75 ppb with largest values occurring between 21 and 05 UTC. GEOS-Chem data is the only product which could replicate the diurnal variability of TROPOZ lidar tropospheric O_3 observations (R = 0.78). The TB-Clim, GEOS-5 FP, and GEOS-Chem products demonstrate moderate high biases (2.2-3.3 ppb) compared to the observations while MERRA2 is consistently low (bias = -5.1 ppb). For comparison of near-surface O_3 values (see Fig. 5d), none of the products sufficiently captured the magnitude and degree of diurnal variability of LMT O_3 at the TROPOZ lidar location. The TB-Clim product displayed a small positive correlation (R = 0.26) and large negative biases (-12.6 ppb), bias standard deviation (6.9 ppb), and RMSE values (14.25 ppb). The GEOS-5 FP and GEOS-Chem models display the lowest bias (negative bias between 7.5 ppb and 7.7 ppb), however, the CTM is more highly correlated (R = 0.92) and resulted in lower bias standard deviations (4.8 ppb) and RMSE values (9.01 ppb). This indicates that while no product reproduced the magnitude or degree of diurnal variability of near-surface O_3 observed by the TROPOZ lidar, the GEOS-Chem CTM does the best job on average.

3.2 Prior O_3 vertical profile impact on TEMPO retrievals

This section focuses on how the TB-Clim, GEOS-5 FP, MERRA2, and GEOS-Chem O_3 profiles impact theoretical TEMPO tropospheric O_3 profile retrievals when applied as the a priori information in Eq. (1). The evaluation is focused on how different sources of a priori impacted the overall accuracy of TEMPO tropospheric O_3 retrievals and the ability to meet the required precision of tropospheric and LMT O_3 observations of 10 ppb (Zoogman et al., 2017). The requirement for TEMPO tropospheric O_3 is that retrieval errors (root square sum of retrieval precision and smoothing errors) or overall biases should be < 10 ppb, and, therefore, we quantify the number of occurrences when total error or bias standard deviation/RMSE exceeds this 10 ppb limit. TEMPO will provide tropospheric and LMT O_3 at high temporal resolution and therefore, X_r values from Eq. (1), using the individual a priori sources, will be evaluated on a daily-averaged and diurnal cycle time scale.

3.2.1 Tropospheric O_3 TEMPO retrievals

Figure 6 shows the time-series of daily-averaged tropospheric and LMT X_r column values and bias calculations when using TB-Clim and model data as a priori information when compared to observed O_3 at all 3 TOLNet sites (statistics in Table 4). When focusing on the accuracy of the theoretical TEMPO retrievals for tropospheric X_r columns (left column in Fig. 6), it can be seen that: 1) X_r values using all a priori profiles are similar and 2) X_r values compare well to observations with tropospheric X_r values typically falling within the 10 ppb bias requirement at all 3 TOLNet locations. From Table 4 it can be seen that daily-averaged tropospheric column biases exceeded the 10 ppb level on 1 and 2 days when using TB-Clim/GEOS-5 FP and MERRA2 data, respectively, as a priori when compared to TROPOZ observations, and for 1 day at the JPL TMF location when using all O_3 products as a priori.

Table 4 illustrates that applying TB-Clim as the a priori resulted in the largest tropospheric column X_r biases and modest bias standard deviations (1.4 ± 2.3 ppb) and the MERRA2 data led to the lowest overall bias and modest bias standard deviation (-0.2 ± 2.5 ppb) at the RO3QET lidar location. Using GEOS-Chem a priori profiles resulted in modest biases and the lowest bias standard deviations (1.0 ± 2.0 ppb) and RMSE values (2.17 ppb). At the TROPOZ system site, the lowest tropospheric column X_r biases and standard deviation were calculated when applying GEOS-Chem as the a priori (-0.5 ± 2.7 ppb). GEOS-5 FP data also resulted in low mean X_r biases but the largest bias standard deviations (-0.6 ± 4.8 ppb) and MERRA2 data led to larger mean X_r biases but lower bias standard deviations (-2.2 ± 4.4 ppb). The use of TB-Clim resulted in modest mean bias and standard deviations (-0.9 ± 4.2 ppb). Finally, at the JPL TMF location all a priori profile sources resulted in average tropospheric column X_r biases of < 1.0 ppb, excluding MERRA2 (bias = -1.7 ppb), with similar bias standard deviations and RMSE values (ranging between 3.0 to 4.0 ppb). Much larger daily variability of tropospheric O_3 was observed at the JPL TMF site compared to the other TOLNet system locations and tropospheric column X_r values from theoretical TEMPO retrievals successfully captured this variability using all the sources of a priori information. These results suggest that TEMPO, using UV+VIS wavelengths, will likely be able to accurately retrieve highly variable tropospheric column O_3 values using a variety of sources of a priori profiles.

3.2.2 LMT O_3 TEMPO retrievals

The third column of Fig. 6 shows that much larger differences in daily-averaged LMT column X_r values were calculated, compared to tropospheric X_r values, when using different sources of a priori in Eq. (1). It can be seen from this figure that at the RO3QET site, daily variability of near-surface O_3 are clearly best captured by LMT X_r values using GEOS-Chem CTM a priori profiles. While the TB-Clim product resulted in LMT X_r values with the smallest mean bias (0.2 ppb), it also led to large RMSE values (5.88 ppb) and the largest bias standard deviations (6.1 ppb) (see Table 4). Table 4 illustrates that LMT column X_r values calculated using CTM a priori profiles had modest mean bias (-2.2 ppb) and the lowest bias standard deviations (2.5 ppb) and RMSE (3.26 ppb). Applying the GEOS-5 FP and MERRA2 model products as a priori profiles resulted in the largest mean biases in LMT X_r values (negative biases ≥ 3.4 ppb) along with largest RMSE values (≥ 6.0 ppb). From an air quality perspective, it is important to note that LMT column X_r values using a priori data other than GEOS-Chem are unable to replicate the larger surface O_3 values occurring in the southeast US (see Fig. 6). A few LMT O_3 accuracy/precision requirement exceedances were calculated at the RO3QET lidar location using all a priori products except for GEOS-Chem predictions. The ability of GEOS-Chem to best reproduce the magnitude of the daily LMT O_3 variability resulted in LMT X_r values with the smallest RMSE and bias standard deviations, no accuracy/precision requirement exceedances, and the best ability to capture the range in daily observed O_3.

At the location of the TROPOZ lidar, it can be seen from Fig. 6 that LMT X_r values, with the use of TB-Clim a priori, are consistently underestimated in comparison to lidar observations. These LMT X_r values have an average negative bias of > 10.0 ppb and largest RMSE values (~13.0 ppb) resulting in 10 days with accuracy/precision requirement exceedances (see Table 4). These large errors are because the a priori profiles provided by TB-Clim are not able to replicate the highly variable vertical O_3 profiles observed at the TROPOZ lidar location. The GEOS-5 FP, MERRA2, and GEOS-Chem models were better able to replicate these highly variable vertical O_3 profiles providing a priori information more accurately representing O_3 in the intermountain west region of the US. This better representation from model data resulted in LMT X_r values with lower negative mean biases (< 6.5 ppb) and smaller RMSE values (< 9.0 ppb) and bias standard deviations (< 6.5 ppb), and also fewer accuracy/precision requirement exceedances. Overall, CTM-predicted a priori information resulted in LMT X_r values with the least bias and bias standard deviation (-4.8 ± 4.8 ppb), RMSE (6.71 ppb), and accuracy/precision exceedances.

At the location of the JPL TMF lidar, much larger daily variability in LMT O_3 mixing ratios were observed during the summer of 2014 compared to the other TOLNet systems. LMT X_r values, using all sources of data as a priori information, had difficulty in replicating this large variability (see Fig. 6). From Table 4, it can be seen that despite relatively low biases for all sources of a priori (< 5.0 ppb), the inability of LMT X_r values to capture the dynamic daily variability resulted in large bias standard deviations and RMSE values (> 12.5 ppb). Furthermore, 6-10 accuracy/precision requirement exceedances out of 26 total days were calculated. Despite 6 error exceedances (the least of all profile products), applying GEOS-Chem predictions as a priori information resulted in the lowest mean biases (1.0 ppb) and RMSE values (12.54 ppb). Typically, large underestimations of LMT X_r values occurred when the lidar observed large O_3 enhancements near the surface and significant overestimations of LMT X_r values were calculated when the lidar observed very large O_3 lamina (>150 ppb) aloft. This indicates that the shape of the a priori

Atmos. Meas. Tech. Discuss., https://doi.org/10.5194/amt-2017-484
Manuscript under review for journal Atmos. Meas. Tech.
Discussion started: 30 January 2018

Atmospheric Measurement Techniques Discussions

O_3 vertical profile used in TEMPO tropospheric O_3 retrievals are very important in order to capture X_r values for both the tropospheric and LMT column and this will be discussed in Sect. 3.2.3.

Figure 6 and Table 4 demonstrate that in general X_r values in the troposphere and near the surface are more accurately retrieved when applying model predictions, and in particular CTM values from GEOS-Chem, at all 3 TOLNet system locations. Also, from this figure it can be seen that in general when large daily-averaged LMT O_3 mixing ratios are observed (here defined as days with daily-averaged LMT O_3 > 65 ppb), which are important for air quality purposes, LMT X_r values display less bias when applying GEOS-Chem a priori profile information compared to all other products. For the 11 days in which daily-averaged LMT O_3 mixing ratios exceeded 65 ppb, 64%, 9%, and 27% of the LMT X_r values had the smallest bias using GEOS-Chem, GEOS-5 FP, and MERRA2 a priori profiles, respectively. This suggests that applying CTM predictions as a priori profile information will allow TEMPO to observe air quality relevant pollution concentrations of LMT O_3 more accurately compared to TB-Clim and models with limited chemistry and emission schemes evaluated during this work.

3.2.3 Importance of a priori vertical profile shape

Figure 7 displays examples of why climatological a priori information in theoretical TEMPO retrievals resulted in large daily-averaged LMT column X_r biases. The first example in Fig. 7a shows the daily-averaged vertical profiles of X_a and X_r with the use of TB-Clim and GEOS-Chem a priori on 08 July 2014 at the JPL TMF site when the lidar observed large LMT O_3 values above EPA NAAQS levels. This case study illustrates how CTMs are more likely to be able to replicate surface O_3 enhancements compared to climatological products. The GEOS-Chem a priori information resulted in more accurate TEMPO X_r values for the tropospheric and LMT O_3 column values. When using GEOS-Chem model predictions as a priori information, TEMPO LMT column X_r retrievals (65.1 ppb) were closer in magnitude to observations (70.2 ppb) compared to when using TB-Clim a priori (54.7 ppb). Furthermore, when using GEOS-Chem a priori information, TEMPO retrievals for the troposphere (65.8 ppb) were also more similar in magnitude to lidar observations (64.2 ppb) compared to using a priori data from TB-Clim (68.2 ppb).

Another example is illustrated in Fig. 7b which shows X_a and X_r when using TB-Clim and GEOS-5 FP predictions as a priori profiles in TEMPO retrievals on 21 August 2014 at the JPL TMF lidar location. On this day, a STE event was likely occurring as tropospheric O_3 mixing ratios were measured to be > 200 ppb between 6-9 km. This case study illustrates how a NRT DAS model, GEOS-5 FP, displayed some ability to replicate the large O_3 lamina in the middle/upper troposphere due to being constrained with upper atmospheric observations. The GEOS-5 FP a priori information resulted in more accurate TEMPO X_r values for the tropospheric and LMT O_3 column values. When using GEOS-5 FP data as a priori information, TEMPO X_r values for tropospheric O_3 of 130.4 ppb compared closely to the JPL TMF lidar observations (135.6 ppb) while TB-Clim data resulted in much lower values (112.4 ppb). However, the large adjustment needed to correct the a priori profiles to match tropospheric column O_3 observations led to noticeable overestimations of TEMPO LMT X_r values. Since the GEOS-5 FP a priori data was able to better replicate the STE event compared to TB-Clim, the LMT X_r overestimation of observed LMT O_3 values (48.8 ppb) is much less when applying GEOS-5 FP (77.6 ppb) than when applying TB-Clim (99.1 ppb). Overall, these results demonstrate that because TEMPO will only have ~1.5 DFS in the troposphere (only ~0.2 DFS in the 0-2 km level), it is important for a priori profiles to match the general shape of observations, throughout the entire troposphere and LMT, in order to accurately retrieve both total tropospheric and LMT O_3 values.

3.2.4 Diurnal cycle of tropospheric TEMPO retrievals

This section focuses on evaluating the ability of TEMPO to retrieve hourly-averaged tropospheric O_3 applying TB-Clim and the GEOS-5 FP, MERRA2, and GEOS-Chem models as a priori profile information. This evaluation was conducted for one day each at the RO3QET and TROPOZ sites where constant lidar measurements were obtained in the troposphere/LMT and near-surface O_3 enhancements with potential air quality relevant impacts were observed. Figure 8 shows the time-series of hourly-averaged tropospheric and LMT column X_r retrievals when using TB-Clim and models as a priori compared to that observed by RO3QET on 07 August 2014 and by TROPOZ on 22 July 2014. This figure also displays the a priori vertical O_3 profiles used in TEMPO retrievals for the hour of largest LMT O_3 observations from the TOLNet systems (20 UTC at the RO3QET location and 22 UTC at the TROPOZ site location).

In comparison to lidar measurements by RO3QET, TEMPO retrievals, with all sources of a priori profiles, are able to reproduce the diurnal pattern of tropospheric and LMT column O_3 values (all R values > 0.98) (see Fig. 8). Table 5 shows that all a priori products allowed TEMPO to retrieve average tropospheric column O_3 with minimal biases, however, GEOS-Chem was the only product which resulted in LMT X_r values comparable to observations. This is because GEOS-Chem a priori profiles allow for more dynamic O_3 retrievals for the entire troposphere and LMT. This is demonstrated by the fact that the daily-mean and standard deviation (1σ) of hourly LMT O_3 from TEMPO using GEOS-Chem a priori information (62.1 ± 5.4 ppb) compared the closest to RO3QET observations (65.2 ± 9.3 ppb). The daily-mean and standard deviations for LMT X_r retrievals, using the other a priori profiles, underpredicted the magnitude and diurnal variability to a higher degree compared to predictions using GEOS-Chem a priori.

Similar results are displayed in Fig. 8 and Table 5 when evaluating the case study at the TROPOZ site location. Once again, TEMPO retrievals with all sources of a priori profiles are generally able to reproduce the diurnal pattern of tropospheric and LMT column O_3 values (all R values > 0.51) but all show large negative biases compared to LMT observations. However, Table 5 shows that GEOS-Chem model a priori data allows TEMPO to retrieve hourly tropospheric and LMT O_3 with the least bias. LMT X_r values using the TB-Clim, GEOS-5 FP, and MERRA2 a priori information displayed too little diurnal variability (nearly a factor of 2 lower standard deviation compared to TEMPO retrievals using GEOS-Chem a priori data) and a consistent underestimate of observations. During both case studies, a priori profile shape was critical for TEMPO retrievals to accurately retrieve both tropospheric and LMT O_3. Figure 8 shows a priori profiles from all products for the hour of each day where largest LMT O_3 observations occurred. This figure further emphasizes that GEOS-Chem CTM simulations are able to better capture the dynamic vertical O_3 profiles observed by the lidars compared to the other a priori profile sources. While the GEOS-Chem X_a profiles underestimate the large LMT O_3 enhancements, the ability to replicate the general shape greatly improves tropospheric and LMT column TEMPO X_r values.

Atmos. Meas. Tech. Discuss., https://doi.org/10.5194/amt-2017-484
Manuscript under review for journal Atmos. Meas. Tech.
Discussion started: 30 January 2018

4 Conclusions

This study evaluated the a priori vertical O_3 profiles currently suggested to be used in TEMPO tropospheric profile retrievals (TB-Clim) and simulated profiles from operational (GEOS-5 FP), reanalysis (MERRA2), and CTM predictions (GEOS-Chem). The spatio-temporal representativeness of the vertical profiles from each product was evaluated using TOLNet lidar observations of tropospheric O_3 during the summer (July-August) of 2014. The TOLNet sites used in this study are situated in areas which represent the southeastern US (RO3QET), intermountain west (TROPOZ), and remote high-elevation locations in the western US (JPL TMF). Because TEMPO will provide high spatial resolution tropospheric (0-10 km) and LMT (0-2 km) O_3 values on an hourly time scale, potential sources of a priori profiles must be able to replicate inter-daily variability and the diurnal cycle of observed vertical tropospheric O_3 profiles.

When evaluating summertime-averaged tropospheric O_3 profiles, it was found that TB-Clim, GEOS-5 FP, MERRA2, and GEOS-Chem data could generally replicate the vertical structure of tropospheric O_3 measured by TOLNet lidars. However, the seasonal/monthly evaluation is insufficient as TEMPO will provide hourly, high spatial resolution, tropospheric and LMT O_3 values. The evaluation of daily-averaged tropospheric and LMT column O_3 values from these products using lidar observations resulted in varying statistical comparisons. Overall, at all 3 TOLNet system locations, GEOS-Chem provided the only data product which consistently captured the inter-daily variability of tropospheric and LMT column O_3 observations. Furthermore, due to the monthly- and zonal-mean nature of TB-Clim, this product was unable to reproduce the inter-daily variability of tropospheric O_3. The ability of the models, in particular GEOS-Chem, to better replicate the temporal variability of O_3 observations led to better statistical comparison to daily-averaged TOLNet data. An important fact demonstrated in this study is that models, primarily GEOS-Chem CTM predictions, displayed better skill in reproducing the largest peaks in daily-averaged near surface O_3 observations which have important implications for air quality. This is partially because GEOS-Chem data best replicated the diurnal cycle of observations of tropospheric and LMT column O_3 from observations. Overall, the GEOS-Chem CTM predictions had the best statistical comparison to daily- and hourly-averaged tropospheric and LMT column O_3 observations.

The importance of different a priori profile products for TEMPO tropospheric O_3 retrievals was evaluated during this study. The results demonstrate that since TEMPO only has ~1.5 DFS in the troposphere (and ~0.2 in the 0-2 km column), the ability of the a priori profile to replicate the actual shape of the "true" O_3 vertical structure (throughout the entire troposphere and LMT) is important in order for the satellite to accurately retrieve both tropospheric column and near surface O_3 values. Although TEMPO X_r values using all a priori data were able to accurately retrieve highly variable column tropospheric O_3 values, there were large differences in LMT X_r values. In general, LMT column X_r values were more accurately retrieved with model a priori profiles, especially with GEOS-Chem predictions. The better performance of TEMPO LMT X_r values, with GEOS-Chem a priori profiles, is because it better reproduces the dynamic vertical structures and inter-daily/diurnal variability of tropospheric O_3. Most importantly from an air quality perspective is that when large daily-averaged LMT O_3 mixing ratios were observed, X_r values near the surface with GEOS-Chem a priori displayed the least bias. Overall, this study suggests that applying a CTM as a priori will likely allow TEMPO retrievals to observe air quality relevant O_3 concentrations more accurately than TB-Clim and other models with limited atmospheric chemistry and emission schemes.

This study is a first step in determining what source of a priori vertical O_3 profiles should be applied to best enhance the ability of TEMPO to retrieve tropospheric and LMT column O_3 in North America. It demonstrates that model simulations, in particular those from a CTM, improve TEMPO tropospheric O_3 retrievals over TB-Clim data. However, there are instances where CTM predictions do not improve TEMPO retrieved values compared to the TB-Clim data. Furthermore, out of the 59 total days of TOLNet observations analyzed during this study, LMT column X_r values using GEOS-Chem a priori profiles show biases greater than the TEMPO 10 ppb accuracy requirement for ~15% of the days. It should be noted that this number of LMT column X_r error exceedances is the least compared to when using all the sources of a priori and greater than a factor of 2 smaller than when applying TB-Clim a priori. The main reason for the majority of error exceedances is because the a priori profiles cannot capture the dynamic vertical O_3 profile observed by the TOLNet lidars. Therefore, further work is needed to identify the source of a priori O_3 profiles for use in TEMPO O_3 retrievals which can best capture the shape of tropospheric O_3 profiles in North America.

Acknowledgements. This work is supported by the TOLNet program within NASA's Science Mission Directorate. X. Liu and P. Zoogman were supported by the NASA Earth Venture Instrument TEMPO project (NNL13AA09C). The authors would also like to thank the Harvard University Atmospheric Chemistry Modeling Group for providing the GEOS-Chem model and the NASA GMAO for providing the GEOS-5 FP and MERRA2 products used during our research. Resources supporting this work were provided by the NASA High-End Computing (HEC) Program through the NASA Advanced Supercomputing (NAS) Division at NASA Ames Research Center. All the authors express gratitude to the support from NASA's Earth Science Division at Ames Research Center. Finally, the views, opinions, and findings contained in this report are those of the authors and should not be construed as an official NASA or United States Government position, policy, or decision.

References

Amos, H. M., Jacob, D. J., Holmes, C. D., Fisher, J. A., Wang, Q., Yantosca, R. M., Corbitt, E. S., Galarneau, E., Rutter, A. P., Gustin, M. S., Steffen, A., Schauer, J. J., Graydon, J. A., St. Louis, V. L., Talbot, R. W., Edgerton, E. S., Zhang, Y., and Sunderland, E. M.: Gas-particle partitioning of atmospheric Hg(II) and its effect on global mercury deposition, Atmos. Chem. Phys., 12, 591-603, https://doi.org/10.5194/acp-12-591-2012, 2012.

Atkinson, R.: Gas-phase Tropospheric Chemistry of Organic Compounds: A Review, Atmos. Environ., 26, 1, 1-41, doi:10.1016/0960-1686(90)90438-S, 1990.

Bacmeister, J. T., Suarez, M. J., and Robertson, F. R.: Rain Re-evaporation, Boundary Layer Convection Interactions, and Pacific Rainfall Patterns in an AGCM, J. Atmos. Sci., 63, 3383-3403, https://doi.org/10.1175/JAS3791.1, 2006.

Bak, J., Liu, X., Wei, J. C., Pan, L. L., Chance, K., and Kim, J. H.: Improvement of OMI ozone profile retrievals in the upper troposphere and lower stratosphere by the use of a tropopause-based ozone profile climatology, Atmos. Meas. Tech., 6, 2239-2254, https://doi.org/10.5194/amt-6-2239-2013, 2013.

Bak, J., Liu, X., Kim, J.-H., Haffner, D. P., Chance, K., Yang, K., and Sun, K.: Characterization and correction of OMPS nadir mapper measurements for ozone profile retrievals, Atmos. Meas. Tech., 10, 4373-4388, https://doi.org/10.5194/amt-10-4373-2017, 2017.

Beer, R.: TES on the aura mission: scientific objectives, measurements, and analysis overview, IEEE Trans. Geosci. Remote Sens., 44, 1102-1105, doi:10.1109/TGRS.2005.863716, 2006.

Bey, I., Jacob, D. J., Yantosca, R. M., Logan, J. A., Field, B., Fiore, A. M., Li, Q., Liu, H., Mickley, L. J., and Schultz, M.: Global modeling of tropospheric chemistry with assimilated meteorology: Model description and evaluation, J. Geophys. Res., 106, 23073-23095, doi:10.1029/2001JD000807, 2001.

Bowman, K. W., Rodgers, C. D., Kulawik, S. S., Worden, J., Sarkissian, E., Osterman, G., Steck, T., Lou, M., Eldering, A., Shephard, M., Worden, H., Lampel, M., Clough, S., Brown, P., Rinsland, C., Gunson, M., and Beer, R.: Tropospheric Emission Spectrometer: retrieval method and error analysis, IEEE Trans. Geosci. Remote Sens., 44, 1297-1307, doi:10.1109/TGRS.2006.871234, 2006.

Cai, Z., Liu, Y., Liu, X., Chance, K., Nowlan, C. R., Lang, R., Munro, R., and Suleiman, R.: Characterization and correction of Global Ozone Monitoring Experiment 2 ultraviolet measurements and application to ozone profile retrievals?, J. Geophys. Res., 117, D07305, doi:10.1029/2011JD017096, 2012.

Chance, K., Liu, X., Suleiman, R. M., Flittner, D. E., Al-Saadi, J., and Janz, S. J.: Tropospheric emissions: Monitoring of pollution (TEMPO), Earth Observing Systems XVIII, Paper 88660D, doi:10.1117/12.2024479, 2013.

Duncan, B. N., Prados, A. I., Lamsal, L. N., Liu, Y., Streets, D. G., Gupta, P., Hilsenrath, E., Kahn, R. A., Nielsen, J. E., Beyersdorf, A. J., Burton, S. P., Fiore, A. M., Fishman, J., Henze, D. K., Hostetler, C. A., Krotkov, N. A., Lee, P., Lin, M. Y., Pawson, S., Pfister, G., Pickering, K. E., Pierce, R. B., Yoshida, Y., and Ziemba, L. D.: Satellite data of atmospheric pollution for US air quality applications: Examples of applications, summary of data end-user resources, answers to FAQs, and common mistakes to avoid, Atmos. Environ., 94, 647-662, doi:10.1016/j.atmosenv.2014.05.061, 2014.

Fishman, J., Bowman, K. W., Burrows, J. P., Richter, A., Chance, K. V., Edwards, D. P., Martin, R. V., Morris, G. A., Pierce, R. B., Ziemke, J. R., Al-Saadi, J. A., Creilson, J. K., Schaack, T. K., and Thompson, A.M.: Remote sensing of tropospheric pollution from space, Bulletin of the American Meteorological Society, 89, 805-821, https://doi.org/10.1175/2008BAMS2526.1, 2008.

Granados-Muñoz, M. J. and Leblanc, T.: Tropospheric ozone seasonal and long-term variability as seen by lidar and surface measurements at the JPL-Table Mountain Facility, California, Atmos. Chem. Phys., 16, 9299-9319, doi:10.5194/acp-16-9299-2016, 2016.

Granados-Muñoz, M. J., Johnson, M. S., and Leblanc, T.: Influence of the North American monsoon on Southern California tropospheric ozone levels during summer in 2013 and 2014, Geophys. Res. Lett., 44, 6431-6439, doi:10.1002/2017GL073375, 2017GL073375, 2017.

Hidy, G. M., Blanchard, C. L., Baumann, K., Edgerton, E., Tanenbaum, S., Shaw, S., Knipping, E., Tombach, I., Jansen, J., and Walters, J.: Chemical climatology of the southeastern United States, 1999-2013, Atmos. Chem. Phys., 14, 11893-11914, doi:10.5194/acp-14-11893-2014, 2014.

Johnson, M. S., Kuang, S., Wang, L., and Newchurch, M. J.: Evaluating Summer-Time Ozone Enhancement Events in the Southeast United States, Atmosphere, 7, 108, doi:10.3390/atmos7080108, 2016.

Kuang, S., Newchurch, M. J., Burris, J., Wang, L., Buckley, P., Johnson, S., Knupp, K., Huang, G., Phillips, D., and Cantrell, W.: Nocturnal ozone enhancement in the lower troposphere observed by lidar, Atmos. Environ., 45, 6078-6084, https://doi.org/10.1016/j.atmosenv.2011.07.038, 2011.

Kuang, S., Newchurch, M. J., Burris, J., and Liu, X.: Ground-based lidar for atmospheric boundary layer ozone measurements, Appl. Opt., 52, 3557-3566, https://doi.org/10.1364/AO.52.003557, 2013.

Kuang, S., Newchurch, M. J., Johnson, M. S., Wang, L., Burris, J., Pierce, R. B., Eloranta, E. W., Pollack, I. B., Graus, M., de Gouw, J., Warneke, C., Ryerson, T. B., Markovic, M. Z., Holloway, J. S., Pour-Biazar, A., Huang, G., Liu, X., and Feng, N.: Summertime tropospheric ozone enhancement associated with a cold front passage due to stratosphere- to-troposphere transport and biomass burning: simultaneous ground-based lidar and airborne measurements, J. Geophys. Res., 122, 1293-1311, doi:10.1002/2016JD026078, 2017.

Langford, A. O., Alvarez, R. J., Brioude, J., Fine, R., Gustin, M. S., Lin, M. Y., Marchbanks, R. D., Pierce, R. B., Sandberg, S. P., Senff, C. J., Weickmann, A. M., and Williams, E. J.: Entrainment of stratospheric air and Asian pollution by the convective boundary layer in the southwestern U.S., J. Geophys. Res., 122, 1312-1337, doi:10.1002/2016JD025987, 2017.

Lelieveld, J. and Dentener, F. J.: What controls tropospheric ozone?, J. Geophys. Res., 105, 3531-3551, doi:10.1029/1999JD901011, 2000.

Lin, M., Fiore, A. M., Horowitz, L. W., Langford, A. O., Oltmans, S. J., Tarasick, D., and Reider, H. E.: Climate variability modulates western US ozone air quality in spring via deep stratospheric intrusions, Nature Communications, 6, 7105, doi:10.1038/ncomms8105, 2015.

Lin, S. J. and Rood, R. B: Multidimensional flux form semi-Lagrangian transport schemes, Mon. Weather Rev., 124, 2046-2070, https://doi.org/10.1175/1520-0493(1996)124<2046:MFFSLT>2.0.CO;2, 1996.

Atmos. Meas. Tech. Discuss., https://doi.org/10.5194/amt-2017-484
Manuscript under review for journal Atmos. Meas. Tech.
Discussion started: 30 January 2018

Atmospheric Measurement Techniques
Discussions

Liu, X., Chance, K., Sioris, C. E., Spurr, R. J. D., Kurosu, T. P., Martin, R. V., and Newchurch, M. J.: Ozone profile and tropospheric ozone retrievals from the Global Ozone Monitoring Experiment: Algorithm description and validation, J. Geophys. Res.-Atmos., 110, D20307, doi:10.1029/2005JD006240, 2005.

Liu, X., Bhartia, P. K., Chance, K., Spurr, R. J. D., and Kurosu, T. P.: Ozone profile retrievals from the Ozone Monitoring Instrument, Atmos. Chem. Phys., 10, 2521-2537, doi:10.5194/acp-10-2521-2010, 2010.

Lock, A. P., Brown, A. R., Bush, M. R., Martin, G. M., and Smith, R. N. B.: A new boundary layer mixing scheme. Part I: Scheme description and single-column model tests, Mon. Weather Rev., 128, 3187-3199, https://doi.org/10.1175/1520-0493(2000)128<3187:ANBLMS>2.0.CO;2, 2000.

Martin, R.: Satellite remote sensing of surface air quality, Atmos. Environ., 42, 7823-7843 http://dx.doi.org/10.1016/j.atmosenv.2008.07.018, 2008.

McPeters, R. D., Labow, G. J., and Logan, J. A.: Ozone climatological profiles for satellite retrieval algorithms, J. Geophys. Res., 112, D05308, doi:10.1029/2005JD006823, 2007.

Molod, A., Takacs, L. L., Suarez, M. J., Bacmeister, J. T., Song, I.-S., and Eichmann, A.: The GEOS-5 Atmospheric General Circulation Model: Mean Climate and Development from MERRA to Fortuna, NASA Tech. Memo. 104606, 28, Tech. Rep. Series on Global Modeling and Data Assimilation, edited by: Suarez, M. J., 117 pp., 2012.

Natraj, V., Liu, X., Kulawik, S., Chance, K., Chatfield, R., Edwards, D. P., Eldering, A., Francis, G., Kurosu, T., Pickering, K., Spurr, R., and Worden, H.: Multi-spectral sensitivity studies for the retrieval of tropospheric and lowermost tropospheric ozone from simulated clear-sky GEO-CAPE measurements, Atmos. Environ., 45, 7151-7165, 2011.

Ott, L. E., Duncan, B. N., Thompson, A. M., Diskin, G., Fasnacht, Z., Langford, A. O., Lin, M., Molod, A. M., Nielsen, J. E., Pusede, S. E.; et al.: Frequency and impact of summertime stratospheric intrusions over Maryland during DISCOVER-AQ (2011): New evidence from NASA's GEOS-5 simulations, J. Geophys. Res. Atmos., 121, doi:10.1002/2015JD024052, 2016.

Putman, W. M. and Lin, S.-J.: Finite-volume transport on various cubed-sphere grids, J. Comput. Phys., 227, 55-78, doi:10.1016/j.jcp.2007.07.022, 2007.

Rienecker, M. M., Suarez, M. J., Todling, R., Bacmeister, J., Takacs, L., Liu, H.-C., Gu, W., Sienkiewicz, M., Koster, R. D., Gelaro, R., Stajner, I., and Nielsen, J. E.: The GEOS-5 Data Assimilation System – Documentation of Versions 5.0.1, 5.1.0, and 5.2.0, NASA/TM-2008-104606, 27, 101 pp, 2008.

Rodgers, C. D.: Inverse Methods for Atmospheric Sounding, World Scientific, River Edge, New Jersey, 2000.

Sauvage, B., Martin, R. V., van Donkelaar, A., Liu, X., Chance, K., Jaeglé, L., Palmer, P. I., Wu, S., and Fu, T.-M.: Remote sensed and in situ constraints on processes affecting tropical tropospheric ozone, Atmos. Chem. Phys., 7, 815-838, https://doi.org/10.5194/acp-7-815-2007, 2007.

Stohl, A., Bonasoni, P., Cristofanelli, P., Collins, W., Feichter, J., Frank, A., Forster, C., Gerasopoulos, E., Gaggeler, H., James, P., Kentarchos, T., Kromp-Kolb, H., Kruger, B., Land, C., Meloen, J., Papayannis, A., Priller, A., Seibert, P., Sprenger, M., Roelofs, G. J., Scheel, H. E., Schnabel, C., Siegmund, P., Tobler, L., Trickl, T., Wernli, H., Wirth, V., Zanis, P., and Zerefos, C.: Stratosphere-troposphere exchange: A review, and what we have learned from STACCATO, J. Geophys. Res., 108(D12), 8516, doi:10.1029/2002JD002490, 2003.

Atmos. Meas. Tech. Discuss., https://doi.org/10.5194/amt-2017-484
Manuscript under review for journal Atmos. Meas. Tech.
Discussion started: 30 January 2018

Atmospheric Measurement Techniques Discussions
Open Access

Sullivan, J. T., McGee, T. J., Thompson, A. M., Pierce, R. B., Sumnicht, G. K., Twigg, L. W., Eloranta, E., and Hoff, R. M.: Characterizing the lifetime and occurrence of stratospheric-tropospheric exchange events in the rocky mountain region using high-resolution ozone measurements, J. Geophys. Res. Atmos., 120, 12410-12424, doi:10.1002/2015JD023877, 2015a.

Sullivan, J. T., McGee, T. J., Leblanc, T., Sumnicht, G. K., and Twigg, L. W.: Optimization of the GSFC TROPOZ DIAL retrieval using synthetic lidar returns and ozonesondes – Part 1: Algorithm validation, Atmos. Meas. Tech., 8, 4133-4143, doi:10.5194/amt-8-4133-2015, 2015b.

U.S. Environmental Protection Agency: Air Quality Criteria for Ozone and Related Photochemical Oxidants (2006 Final), U.S. Environmental Protection Agency, Washington, DC, EPA/600/R-05/004aF-cF, 2006.

U.S. Environmental Protection Agency. National Ambient Air Quality Standards for Ozone - Final Rule, Federal Register 80, 65292-65468, available at https://www.gpo.gov/fdsys/pkg/FR-2015-10-26/pdf/2015-26594.pdf, 2015.

Vu, K. T., Dingle, J. H., Bahreini, R., Reddy, P. J., Apel, E. C., Campos, T. L., DiGangi, J. P., Diskin, G. S., Fried, A., Herndon, S. C., Hills, A. J., Hornbrook, R. S., Huey, G., Kaser, L., Montzka, D. D., Nowak, J. B., Pusede, S. E., Richter, D., Roscioli, J. R., Sachse, G. W., Shertz, S., Stell, M., Tanner, D., Tyndall, G. S., Walega, J., Weibring, P., Weinheimer, A. J., Pfister, G., and Flocke, F.: Impacts of the Denver Cyclone on regional air quality and aerosol formation in the Colorado Front Range during FRAPPÉ 2014, Atmos. Chem. Phys., 16, 12039-12058, doi:10.5194/acp-16-12039-2016, 2016.

Wang, Y. H., Jacob, D. J., and Logan, J. A: Global simulation of tropospheric O3-NOx-hydrocarbon chemistry: 1. Model formulation, J. Geophys. Res., 103, 10713-10725, doi:10.1029/98JD00158, 1998.

Wargan, K., Pawson, S., Olsen, M. A., Witte, J. C., Douglass, A. R., Ziemke, J. R., Strahan, S. E., and Nielsen, J. E.: The global structure of upper troposphere-lower stratosphere ozone in GEOS-5: A multiyear assimilation of EOS Aura data, J. Geophys. Res. Atmos., 120, 2013-2036, doi:10.1002/2014JD022493, 2015.

Worden, H. M., Logan, J. A., Worden, J. R., Beer, R., Bowman, K., Clough, S. A., Eldering, A., Fisher, B. M., Gunson, M. R., Herman, R. L., Kulawik, S. S., Lampel, M. C., Luo, M., Megretskaia, I. A., Osterman, G. B., and Shephard, M.W.: Comparisons of Tropospheric Emission Spectrometer (TES) ozone profiles to ozonesondes: Methods and initial results, J. Geophys. Res., 112, D03309, doi:10.1029/2006JD007258, 2007.

Wu, W.-S., Purser, R. J., and Parrish, D. F.: Three-dimensional variational analysis with spatially inhomogeneous covariances, Mon. Wea. Rev., 130, 2905-2916, https://doi.org/10.1175/1520-0493(2002)130<2905:TDVAWS>2.0.CO;2, 2002.

Zoogman, P., Jacob, D. J., Chance, K., Liu, X., Lin, M., Fiore, A., and Travis, K.: Monitoring high-ozone events in the US Intermountain West using TEMPO geostationary satellite observations, Atmos. Chem. Phys., 14, 6261-6271, https://doi.org/10.5194/acp-14-6261-2014, 2014.

Zoogman, P., Liu, X., Suleiman, R., Pennington, W., Flittner, D., Al-Saadi, J., Hilton, B., Nicks, D., Newchurch, M., Carr, J., Janz, S., Andraschko, M., Arola, A., Baker, B., Canova, B., Miller, C. C., Cohen, R., Davis, J., Dussault, M., Edwards, D., Fishman, J., Ghulam, A., Abad, G. G., Grutter, M., Herman, J., Houck, J., Jacob, D., Joiner, J., Kerridge, B., Kim, J., Krotkov, N., Lamsal, L., Li, C., Lindfors, A., Martin, R., McElroy, C., McLinden, C., Natraj, V., Neil, D., Nowlan, C., O'Sullivan, E., Palmer, P., Pierce, R., Pippin, M., Saiz-Lopez, A., Spurr, R., Szykman, J., Torres, O., Veefkind, J., Veihelmann, B., Wang, H., Wang, J., and Chance, K.: Tropospheric emissions: Monitoring of pollution (TEMPO), J. Quant. Spectrosc. Ra., 186, 17-39, https://doi.org/10.1016/j.jqsrt.2016.05.008, 2017.

Atmos. Meas. Tech. Discuss., https://doi.org/10.5194/amt-2017-484
Manuscript under review for journal Atmos. Meas. Tech.
Discussion started: 30 January 2018

Atmospheric Measurement Techniques Discussions

Tables

Table 1. Information about the TOLNet systems applied during this study.

System Name	Latitude (°N)	Longitude (°W)	Elevation (m)[a]	# of observations[b]
TROPOZ	40.6	105.1	1569.0	21
JPL TMF	34.4	117.7	2285.0	26[c]
RO3QET	34.7	86.6	206.0	12[d]

[a]Elevation of the topography above sea level.
[b]Number of days of lidar observations between July - August 2014.
[c]JPL TMF lidar observations only taken during nighttime hours between July-August 2014.
[d]RO3QET lidar observations only taken from the surface to ~5 km between July-August 2014.

Atmos. Meas. Tech. Discuss., https://doi.org/10.5194/amt-2017-484
Manuscript under review for journal Atmos. Meas. Tech.
Discussion started: 30 January 2018

Atmospheric Measurement Techniques Discussions

Table 2. Time-series evaluation of TB-Clim, GEOS-5 FP, MERRA2, and GEOS-Chem daily-averaged tropospheric and LMT column O_3 with the RO3QET, TROPOZ and JPL TMF lidars. The statistics include correlation (R), mean bias, bias standard deviation (1σ), and root mean squared error (RMSE).

RO3QET	**TB-Clim**	**GEOS-5 FP**	**MERRA2**	**GEOS-Chem**
Tropospheric Column O_3 (0-5 km)				
Correlation (R)	-0.09	0.23	-0.10	0.61
Bias ± 1σ (ppb)	3.7 ± 6.0	2.8 ± 5.6	-0.7 ± 5.8	1.7 ± 4.2
RMSE (ppb)	6.81	6.14	5.61	4.34
LMT Column O_3 (0-2 km)				
Correlation (R)	-0.68	0.03	-0.19	0.83
Bias ± 1σ (ppb)	2.9 ± 9.7	-2.9 ± 8.5	-4.9 ± 8.0	-1.3 ± 4.4
RMSE (ppb)	9.75	8.65	9.06	4.39
TROPOZ	**TB-Clim**	**GEOS-5 FP**	**MERRA2**	**GEOS-Chem**
Tropospheric Column O_3 (0-10 km)				
Correlation (R)	-0.09	0.26	0.38	0.82
Bias ± 1σ (ppb)	2.2 ± 9.7	3.3 ± 10.0	-4.6 ± 9.1	2.4 ± 6.0
RMSE (ppb)	9.73	10.33	9.99	6.30
LMT Column O_3 (0-2 km)				
Correlation (R)	-0.15	-0.09	-0.18	0.47
Bias ± 1σ (ppb)	-11.1 ± 7.5	-4.4 ± 7.3	-7.4 ± 7.4	-6.7 ± 6.2
RMSE (ppb)	13.23	8.43	10.33	8.93
JPL TMF	**TB-Clim**	**GEOS-5 FP**	**MERRA2**	**GEOS-Chem**
Tropospheric Column O_3 (0-10 km)				
Correlation (R)	-0.35	0.76	0.80	0.72
Bias ± 1σ (ppb)	0.3 ± 18.7	-5.0 ± 13.8	-10.6 ± 13.4	-0.5 ± 14.6
RMSE (ppb)	18.38	14.41	16.86	14.29
LMT Column O_3 (0-2 km)				
Correlation (R)	-0.53	-0.21	0.22	0.49
Bias ± 1σ (ppb)	3.3 ± 13.6	-2.4 ± 12.7	-4.0 ± 11.7	0.9 ± 10.4
RMSE (ppb)	13.72	12.68	12.14	10.24

683 **Table 3. Time-series evaluation of the TB-Clim, GEOS-5 FP, MERRA2, and GEOS-Chem hourly-averaged**
684 **tropospheric and LMT column O_3 with the RO3QET, TROPOZ and JPL TMF lidars. The statistics include**
685 **correlation (R), mean bias, bias standard deviation (1σ), and root mean squared error (RMSE).**

RO3QET	**TB-Clim**	**GEOS-5 FP**	**MERRA2**	**GEOS-Chem**
Tropospheric Column O_3 (0-5 km)				
Correlation (R)	-0.54	-0.55	-0.51	0.68
Bias ± 1σ (ppb)	3.5 ± 1.4	2.6 ± 1.6	-1.2 ± 1.5	2.1 ± 1.1
RMSE (ppb)	3.77	2.98	1.86	2.37
LMT Column O_3 (0-2 km)				
Correlation (R)	0.20	0.55	-0.43	0.76
Bias ± 1σ (ppb)	1.9 ± 3.9	-3.3 ± 3.6	-5.9 ± 4.0	0.3 ± 2.6
RMSE (ppb)	4.20	4.73	7.04	2.45
TROPOZ	**TB-Clim**	**GEOS-5 FP**	**MERRA2**	**GEOS-Chem**
Tropospheric Column O_3 (0-10 km)				
Correlation (R)	-0.07	-0.38	-0.56	0.78
Bias ± 1σ (ppb)	2.6 ± 2.5	3.3 ± 2.6	-5.1 ± 3.2	2.2 ± 1.7
RMSE (ppb)	3.57	4.17	6.00	2.74
LMT Column O_3 (0-2 km)				
Correlation (R)	0.26	0.76	0.67	0.92
Bias ± 1σ (ppb)	-12.6 ± 6.9	-7.5 ± 6.6	-9.6 ± 6.9	-7.7 ± 4.8
RMSE (ppb)	14.25	9.91	11.70	9.01

686

Atmos. Meas. Tech. Discuss., https://doi.org/10.5194/amt-2017-484
Manuscript under review for journal Atmos. Meas. Tech.
Discussion started: 30 January 2018

Atmospheric Measurement Techniques
Discussions

Table 4. Time-series evaluation of daily-averaged X_r predictions using the TB-Clim, GEOS-5 FP, MERRA2, and GEOS-Chem data as a priori information in theoretical TEMPO retrievals of tropospheric and LMT column O_3 values with RO3QET, TROPOZ and JPL TMF lidars. The statistics include mean bias, bias standard deviation (1σ), root mean squared error (RMSE), and the number of occurrences where error exceeds 10 ppb.

RO3QET	**TB-Clim**	**GEOS-5 FP**	**MERRA2**	**GEOS-Chem**
Tropospheric Column O_3 (0-5 km)				
Bias ± 1σ (ppb)	1.4 ± 2.3	1.3 ± 2.7	-0.2 ± 2.5	1.0 ± 2.0
RMSE (ppb)	2.66	2.91	2.43	2.17
10 ppb error exceedance	0	0	0	0
LMT Column O_3 (0-2 km)				
Bias ± 1σ (ppb)	0.2 ± 6.1	-3.8 ± 5.5	-3.4 ± 5.1	-2.2 ± 2.5
RMSE (ppb)	5.88	6.44	5.97	3.26
10 ppb error exceedance	1	3	2	0
TROPOZ	**TB-Clim**	**GEOS-5 FP**	**MERRA2**	**GEOS-Chem**
Tropospheric Column O_3 (0-10 km)				
Bias ± 1σ (ppb)	-0.9 ± 4.2	-0.6 ± 4.8	-2.2 ± 4.4	-0.5 ± 2.7
RMSE (ppb)	4.21	4.72	4.85	2.66
10 ppb error exceedance	1	1	2	0
LMT Column O_3 (0-2 km)				
Bias ± 1σ (ppb)	-11.4 ± 6.2	-6.4 ± 6.3	-5.1 ± 5.9	-4.8 ± 4.8
RMSE (ppb)	12.95	8.85	7.67	6.71
10 ppb error exceedance	10	6	4	3
JPL TMF	**TB-Clim**	**GEOS-5 FP**	**MERRA2**	**GEOS-Chem**
Tropospheric Column O_3 (0-10 km)				
Bias ± 1σ (ppb)	-0.2 ± 4.0	-0.8 ± 3.1	-1.7 ± 3.0	-0.3 ± 3.3
RMSE (ppb)	3.97	3.14	3.42	3.29
10 ppb error exceedance	1	1	1	1
LMT Column O_3 (0-2 km)				
Bias ± 1σ (ppb)	3.1 ± 14.8	1.9 ± 13.7	4.8 ± 12.6	1.0 ± 12.7
RMSE (ppb)	14.87	13.57	13.27	12.54
10 ppb error exceedance	9	8	10	6

694 695 696 697 698 **Table 5. Time-series evaluation of hourly-averaged TOLNet observations and X_r predictions using the TB-Clim, GEOS-5 FP, MERRA2, and GEOS-Chem data as a priori information in theoretical TEMPO retrievals of tropospheric and LMT column O_3 values at the location of RO3QET (07 August, 2014) and TROPOZ (22 July, 2014). The statistics include mean, min/max, and standard deviation (1σ) from observations and theoretical TEMPO retrievals.**

RO3QET 07 August, 2014	**TOLNet**	**TB-Clim**	**GEOS-5 FP**	**MERRA2**	**GEOS-Chem**
Tropospheric Column O_3 (0-5 km)					
Mean (ppb)	60.7	59.8	59.5	59.0	59.5
Max/Min (ppb)	67.5/56.4	64.7/56.8	64.1/56.9	63.8/56.1	65.1/55.5
Std. Dev. (ppb)	3.62	2.63	2.35	2.55	3.18
LMT Column O_3 (0-2 km)					
Mean (ppb)	65.2	56.5	53.4	53.1	62.1
Max/Min (ppb)	79.4/54.3	62.6/52.5	59.4/49.8	59.4/48.8	70.6/54.6
Std. Dev. (ppb)	9.27	3.41	3.33	3.67	5.38
TROPOZ 22 July, 2014	**TOLNet**	**TB-Clim**	**GEOS-5 FP**	**MERRA2**	**GEOS-Chem**
Tropospheric Column O_3 (0-10 km)					
Mean (ppb)	50.5	52.4	52.2	50.7	50.3
Max/Min (ppb)	55.8/46.3	55.7/49.2	55.5/49.0	53.3/47.7	53.3/47.3
Std. Dev. (ppb)	3.25	2.60	2.52	2.06	2.40
LMT Column O_3 (0-2 km)					
Mean (ppb)	75.0	44.3	49.9	51.2	56.3
Max/Min (ppb)	97.0/58.6	47.5/41.3	54.3/45.6	54.9/47.3	66.4/47.8
Std. Dev. (ppb)	12.77	2.27	2.96	2.81	5.93

699

700

Atmos. Meas. Tech. Discuss., https://doi.org/10.5194/amt-2017-484
Manuscript under review for journal Atmos. Meas. Tech.
Discussion started: 30 January 2018

Atmospheric Measurement Techniques
Discussions
Open Access

Figures

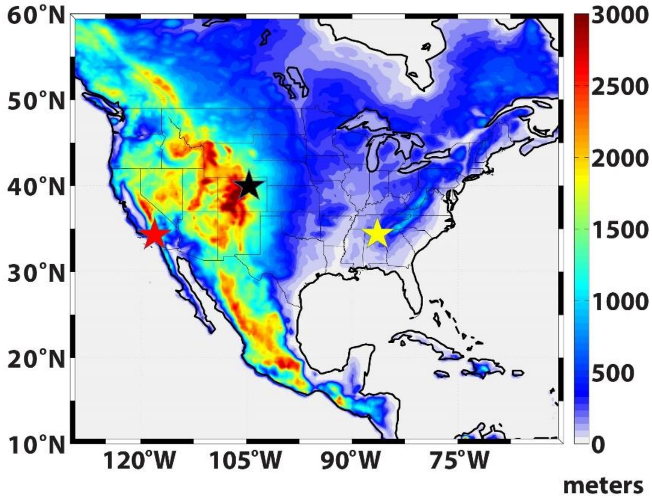

Figure 1. Location of the GSFC TROPOZ (black star), JPL TMF (red star), and the UAH RO3QET (yellow star) TOLNet systems during the summer of 2014. The locations are overlaid on the topographic heights (meters) from the GEOS-5 model.

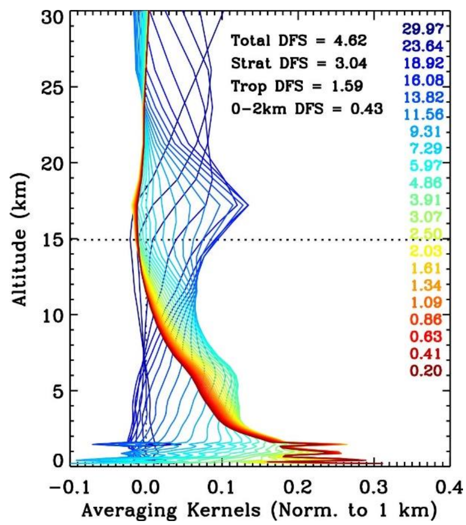

Figure 2. Simulated TEMPO O_3 retrieval AK matrix (normalized to 1 km layer) from joint UV+VIS measurements (290-345 nm, 540-650 nm) from the surface to 30 km above ground level used at the UAH TOLNet site during August at 20 UTC. The AK lines are for individual vertical levels (km above ground level), with the colors ranging from red to blue representing vertical levels from surface air to ~30 km. The legend presents the DFS for the total (Total), stratosphere (Strat), troposphere (Trop), and 0-2 km columns.

Atmos. Meas. Tech. Discuss., https://doi.org/10.5194/amt-2017-484
Manuscript under review for journal Atmos. Meas. Tech.
Discussion started: 30 January 2018

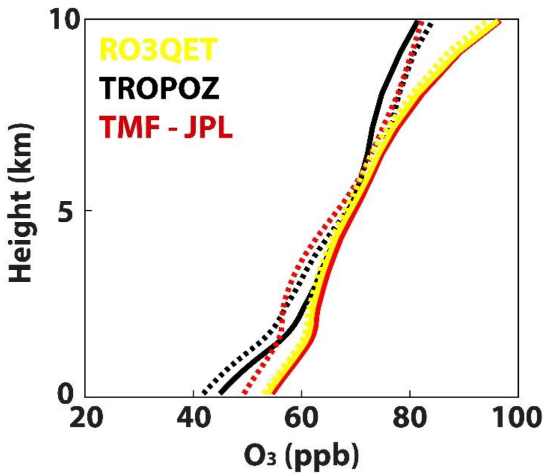

Figure 3. Monthly-averaged vertical profiles of O_3 (ppb) from TB-Clim data at the location of the RO3QET (yellow lines), TROPOZ (black lines), and JPL TMF (red lines) TOLNet systems for July (solid lines) and August (dashed lines). The monthly-averages are derived using the hourly TB-Clim data during the hours/days of observations obtained at each location.

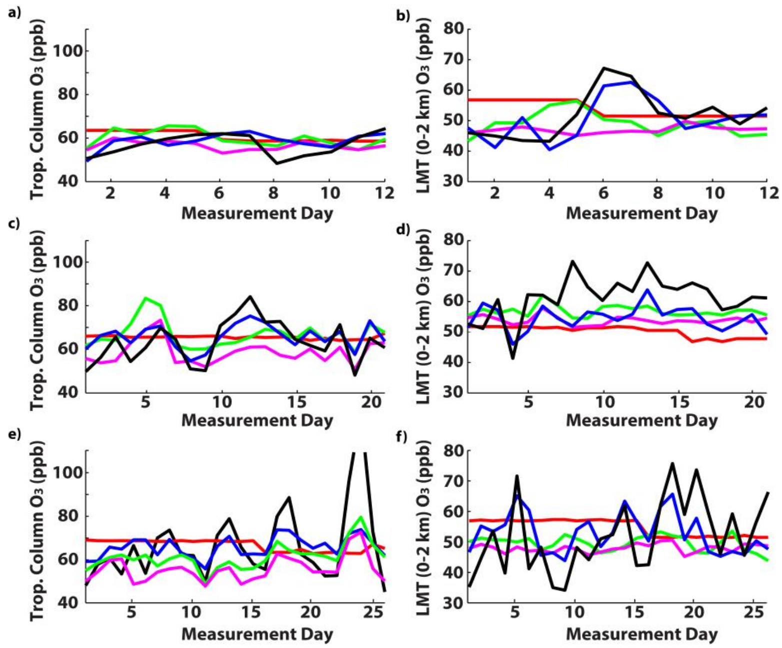

Figure 4. Time-series of daily-averaged tropospheric column (0-10 km) O_3 (ppb) from TB-Clim (red line), GEOS-5 FP (green line), MERRA2 (magenta line), and GEOS-Chem (blue line) compared to TOLNet (black line) at the locations of a) RO3QET, c) TROPOZ, and e) JPL TMF. Panels b), d), and f) are similar but for the comparison of LMT column (0-2 km) O_3.

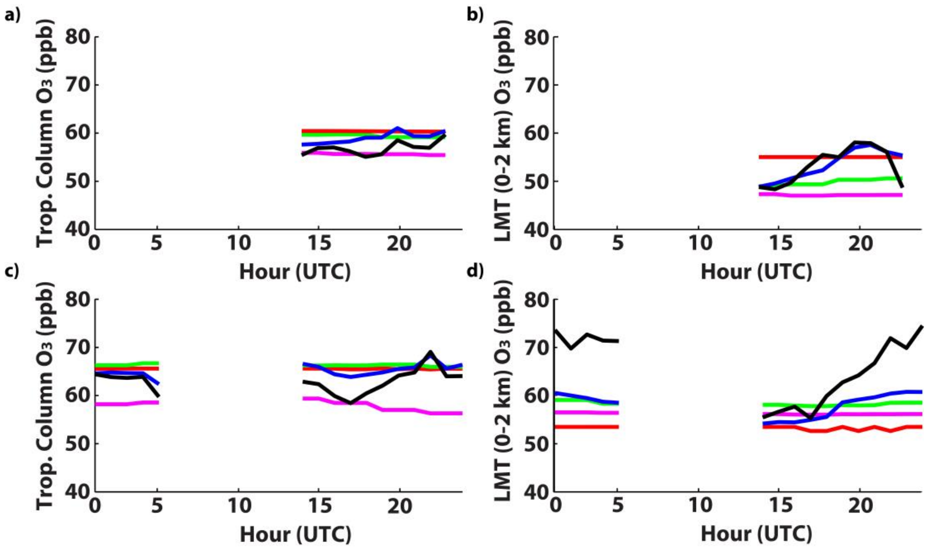

Figure 5. Diurnal time-series of hourly-averaged tropospheric column (0-10 km) O_3 (ppb) from TB-Clim (red line), GEOS-5 FP (green line), MERRA2 (magenta line), and GEOS-Chem (blue line) compared to TOLNet (black line) at the locations of a) RO3QET and c) TROPOZ. Panels b) and d) are similar but for the comparison of LMT column (0-2 km) O_3. The times of missing data are hours where no TOLNet observations were taken during the summer of 2014.

Atmos. Meas. Tech. Discuss., https://doi.org/10.5194/amt-2017-484
Manuscript under review for journal Atmos. Meas. Tech.
Discussion started: 30 January 2018

Atmospheric Measurement Techniques Discussions

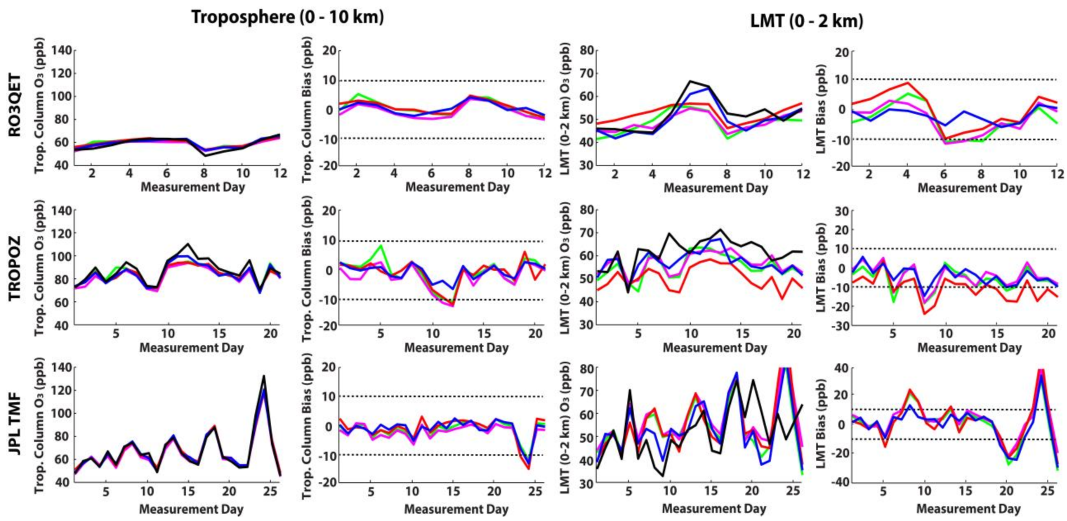

Figure 6. Time-series of daily-averaged tropospheric and LMT column X_r and bias values (ppb) when using TB-Clim (red line), GEOS-5 FP (green line), MERRA2 (magenta line), and GEOS-Chem (blue line) as the a priori when compared to observed O_3 by TOLNet (black line) at the locations of RO3QET (top row), TROPOZ (middle row), and JPL TMF (bottom row). The dashed black lines represent the 10 ppb precision/accuracy requirement for TEMPO O_3 retrievals.

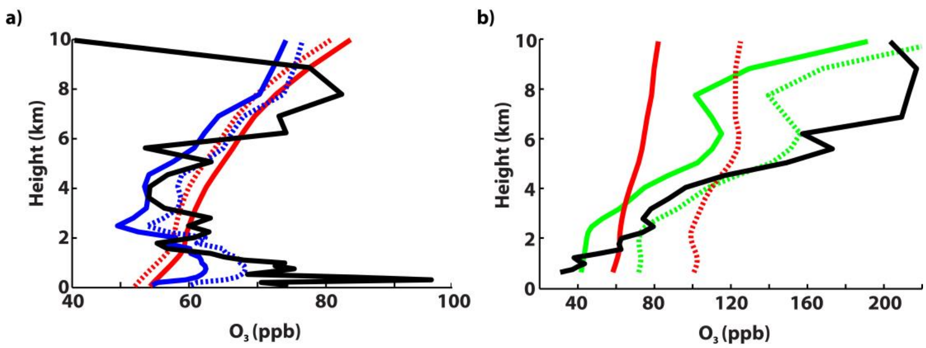

741

742 **Figure 7. Vertical profiles of a) daily-averaged X_a (solid line) and X_r (dashed line) O_3 values when applying**
743 **TB-Clim (red line) and GEOS-Chem (blue line) as a priori information in TEMPO retrievals compared to**
744 **TOLNet (black line) at the locations of the JPL TMF lidar on 08 July, 2014. Panel b) shows daily-averaged X_a**
745 **and X_r O_3 values when applying TB-Clim (red line) and GEOS-5 FP (green line) as a priori information in**
746 **TEMPO retrievals compared to TOLNet (black line) at the locations of the JPL TMF lidar on 21 August, 2014.**

747

Atmos. Meas. Tech. Discuss., https://doi.org/10.5194/amt-2017-484
Manuscript under review for journal Atmos. Meas. Tech.
Discussion started: 30 January 2018

Atmospheric Measurement Techniques
Discussions

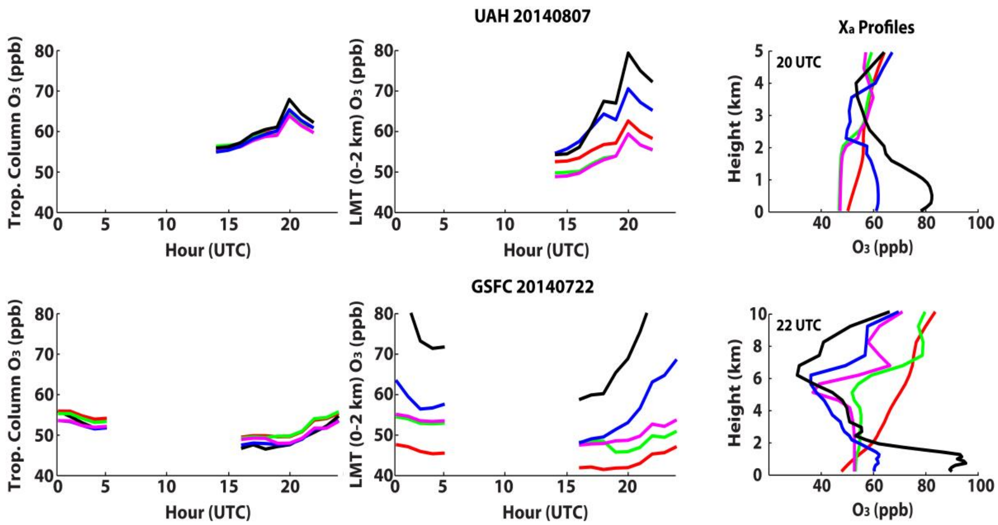

Figure 8. Diurnal time-series of hourly-averaged tropospheric (0-10 km) and LMT (0-2 km) column X_r O_3 (ppb) values with a priori from TB-Clim (red line), GEOS-5 FP (green line), MERRA2 (magenta line), and GEOS-Chem (blue line) compared to TOLNet (black line) at the locations of RO3QET location on 07 August 2014 (top row) and TROPOZ on 22 July 2014 (bottom row). The hourly-averaged a priori vertical profiles are also presented (right column) along with TOLNet (black line) for the hour of largest LMT O_3 observed by TOLNet in the time-series.